JREE: Vol. 9, No. 2, (Spring 2022) 49-58

Journal of Renewable Energy and Environment

Journal Homepage: www.jree.ir

Materials and Energy Research Center

MERC

Research Article

Multi-Response Optimization of Tubular Microbial Fuel Cells Using Response Surface Methodology (RSM)

Maryam Keshavarz [a], Davod Mohebbi-Kalhori [a,b*], Vajihe Yousefi [a]

[a] *Department of Chemical Engineering, Faculty of Engineering, University of Sistan and Baluchestan, Zahedan, Sistan and Baluchestan, Iran.*
[b] *University of Sistan and Baluchestan Central Laboratory, Zahedan, Sistan and Baluchestan, Iran.*

PAPER INFO

Paper history:
Received: 14 June 2021
Revised in revised form: 03 January 2022
Scientific Accepted: 11 October 2021
Published: 19 March 2022

Keywords:
Microbial Fuel Cell,
Response Surface Methodology (RSM),
Separator-Electrode Assembly,
J-Cloth,
Nylon-Cloth,
Domestic Wastewater Treatment

ABSTRACT

Response surface methodology is employed to statistically identify the significance of three parameters of separator assembly arrangement, wastewater flow rate, and relative flow patterns of anode and cathode influencing the generation of power and coulombic efficiency of Microbial Fuel Cells (MFCs). Three different assemblies of Nylon-Cloth (NC), artificial rayon cloth as Absorbent Layer (AL), and J-Cloth (JC) were investigated as proton exchange mediums instead of common expensive polymeric membranes. Statistical analyses (ANOVA) revealed that although the addition of the AL after the JC layer had no significant impact on the enhancement of maximum power density, it could improve the coulombic efficiency of the MFCs by 15 %, owing to the crucial impact of oxygen permeability control between the MFC chambers. In the counter-current flow pattern, higher trans-membrane pressure and more oxygen concentration differences diminished the MFC performance and marked the importance of efficient separator layer arrangement, compared to co-current influents. The maximum power density of 285.89 mW/m^2, the coulombic efficiency of 4.97 %, and the internal resistance of 323.9 Ω were achieved for the NC-JC-Al arrangement in the co-current mode along with the flow rate of 6.9 ml/min. The higher the flow rate of influent wastewater, the higher the performance of the MFCs.

https://doi.org/10.30501/jree.2022.290677.1218

1. INTRODUCTION

The know-how of electricity production processes from renewable resources has been known for many years; however, the critical need for the development of more practical and viable utilization of novel renewable technologies has been perceived on a global scale [1-4]. Microbial Fuel Cell (MFC) is known as a novel, useful and eco-friendly approach that not only generates clean energy but also solves the problems concerned with the contamination of water sources by treating the polluted waters and wastewaters [5-7]. Generally, Each MFC system consists of an anode chamber, a cathode chamber, and a membrane for exchanging the produced protons and separating the anode and cathode from each other [8, 9]. The source of electrical energy in MFCs is bacteria that reside in the biomass [10-12] and use the microbial-catalyzed redox reactions to produce bio-electricity directly [13]. The substrates are oxidized using the microorganisms presented in the wastewater medium and this results in electron and proton generation [11, 13]. Transfer of protons through the separator, followed by the combination of electrons with protons and oxygen results in the generation of water on the cathode surface. Electricity is simultaneously produced by the transportation of electrons through the external circuit [14]. By improving the performance of the MFC as well as reducing their component costs, it can be a promising source of energy generation in the future [15, 16].

Various parameters affecting the performance and overall cost of MFCs include their designs, operating conditions, and types of materials used for electrodes and separators. However, it seems that among many obstacles against the MFC scale-up, the challenge of finding an appropriate proton exchange medium that has low cost, efficient proton transferability, and long-term stability is of great importance. In this regard, many innovative separators have been used such as porous fabrics, nylon meshes, glass fiber, J-cloth, and ceramics, which are not ion-selective and the species are transferred based on their pore size [17-24]. Generally, these size-selective separators have a higher proton transfer capability and better applicability than the common Ion Exchange Membranes (IEM). However, higher oxygen and substrate permeation through these coarse-pore separators is their most important shortcoming [25, 26], especially for Separator-Electrode Assembly (SEA) design of MFCs whose electrodes were closely placed on both sides of the separator

*Corresponding Author's Email: davoodmk@eng.usb.ac.ir (D. Mohebbi-Kalhori)
URL: https://www.jree.ir/article_147027.html

Please cite this article as: Keshavarz, M., Mohebbi-Kalhori, D. and Yousefi, V., "Multi-response optimization of tubular microbial fuel cells using response surface methodology (RSM)", ***Journal of Renewable Energy and Environment (JREE)***, Vol. 9, No. 2, (2022), 49-58. (https://doi.org/10.30501/jree.2022.290677.1218).

[27, 28]. To address this problem and take advantage of different genera's benefits, an assemblage of various size-selective separators was utilized as a proton exchange medium in some studies. For instance, in our previous work, three layers of NC, JC, and Glass Fiber (GF) have been successfully assembled as a separator of the continuous tubular microbial fuel cell [20]. NC layer was placed next to the anode chamber and JC and GF layers were assembled afterward in three arrangements. Though implementation of GF layer after the JC layer increased the electrode thickness due to its relatively high thickness (4 mm), it could block the excess oxygen crossing between the chambers and hence, improve the power and current densities remarkably. Moreover, the effect of two other important parameters including Hydraulic Retention Time (HRT) and relative flow patterns of influent anode and cathode electrolytes were investigated and optimized separately [20].

However, this study with many other industrial and laboratory scale processes was conventionally investigated using One-Factor-At-a-Time (OFAT) optimization method, which was only functionalized for the examination of single varied factors and did not include the interaction of various factors. To solve this problem, statistical Response Surface Methodology (RSM) can be used to build an empirical model by analyzing the affecting parameters as well as their interactions. This useful technique has also become more popular in biochemical fields, where a distinct mechanistic model cannot be easily formulated [29-32].

Therefore, in this work, the effects of three important factors of separator layers arrangement, wastewater flow rate (or HRT), and the anolyte and catholyte flow patterns were statistically optimized by using RSM according to D-optimal design.

As the first categorical factor, three different combinations of cost-effective porous layers, i.e., including nylon cloth (NC), J-cloth (JC), and the absorbent layer of artificial rayon (AL), were selected to find the best design of Separator-Electrode Assembly (SEA) for continuous tubular MFCs. Two flow patterns of anolyte versus catholyte (co-current and counter-current) were also investigated simultaneously. The flow rate of influent wastewater to the anode chamber, the only numeric factor of this design, was controlled between as 2.9 and 6.9 ml/min at 5 levels. On the other hand, the Maximum Power Density (MPD) and Coulombic Efficiency (CE) of each experiment were adopted as two responses of this statistical optimization. There are many types of research on the optimization of microbial fuel cell's operational conditions as well as those types of researches that focused absolutely on finding appropriate low-cost separators. However, to the best of our knowledge, this study is the first one that statistically investigates and optimizes different separator-electrode assemblies as well as prominent operational parameters along with their interactive effects.

2. MATERIALS AND METHODS

2.1. MFC construction

The MFC designs are almost similar to our previous study except for minor design differences including use of brass valves instead of plastic cones for input and output sections of the anode and cathode chambers. Moreover, a new absorbent fabric layer is implemented instead of glass fiber in the proton exchange layers [20]. The schematic design along with visual preparation steps of the tubular MFCs is given in Figure 1. The two-chambered MFCs consist of the inner cylindrical anode chamber (diameter = 3 cm and long = 30 cm) and the outer coaxial cathode chamber (diameter = 6 cm and long =30 cm). The anode surface was perforated using a drill (100 homogenously pores, each diameter 3 mm) for crossing the protons (surface area of 0.0007 m^2).

The separators used in the MFCs as the proton exchange medium composed of Nylon Cloth (NC, 0.5 mm thick, 70 µm pore diameter, and polyamide material), J-cloth (JC, 1 mm thick, Canada), and artificial rayon cloth as the absorbent layer (AL, 3 mm thick) in three different arrangements.

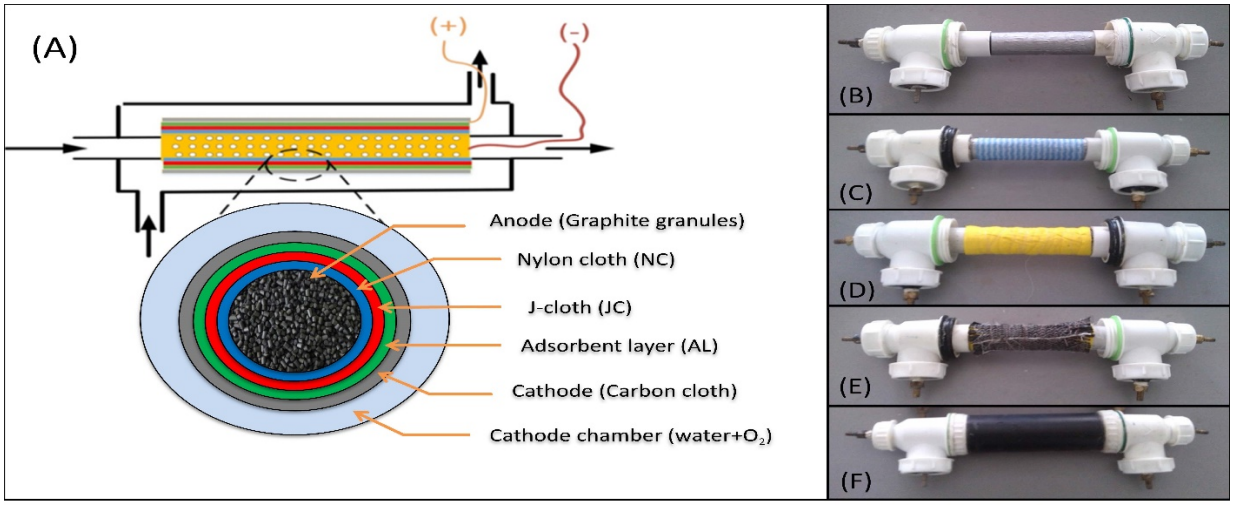

Figure 1. (A) schematic presentation of the tubular MFCs along with their cross-section details, (B) the assembled NC (thickness of 0.5 mm) over the perforated anode tube, (C) the J-cloth layer (1 mm thickness) wrapped around the nylon cloth, (D) the absorbent layer (3 mm thickness) over the previous layers, (E) the carbon cloth cathode, and (F) the completed MFC with an outer PVC tube as cathode chamber

The cathode electrode was made of carbon cloth (11 cm width and 13 cm length) wrapped on the applied multilayer separator (Figure 1E) and tightened using a thin pure copper wire as a collector for produced current. Granular graphite with an average diameter of 4 mm, the porosity of 9.39 %, and density of 1.77 g/cm^3 was used as an anode electrode accompanied by the spiral aluminum strip with a width of 0.9 cm and a length of 60 cm as the anode current collector, which was embedded into the anode compartment.

Fresh wastewater was continuously supplied from the septic tank of the sewage treatment plant of the University of Sistan and Baluchestan as anode electrolyte by a pump. Oxygen saturated tap water as catholyte was continuously fed into the cathode compartment. All experiments were triplicated by 3 similar MFCs in the same conditions, in which the temperature was controlled in the MFC containing chamber at 37 ºC, as depicted in Figure 2.

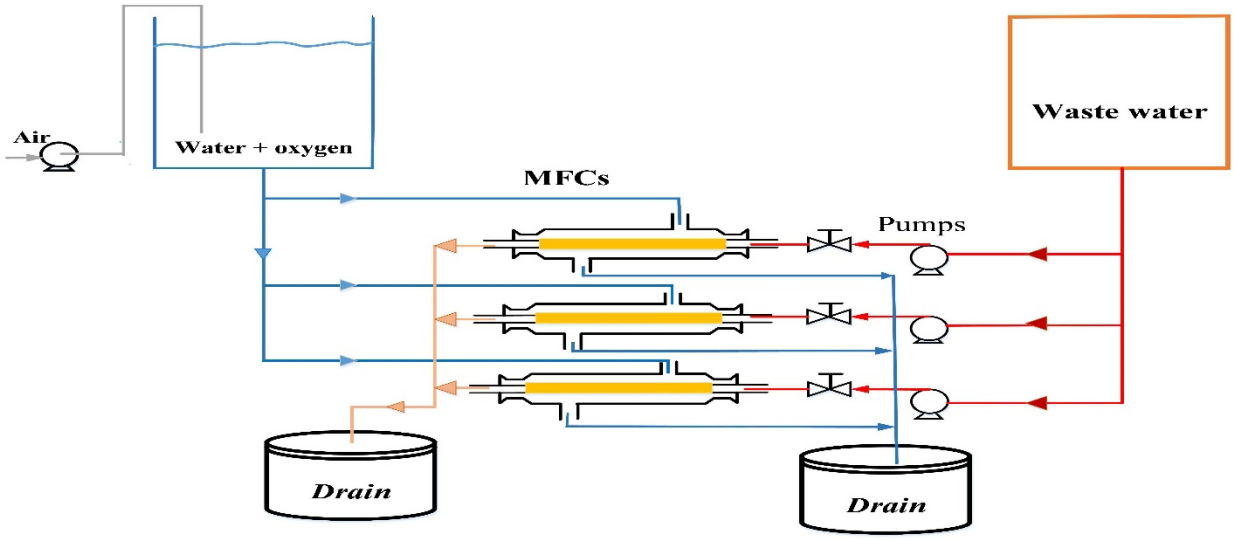

Figure 2. The process diagram of the experimental setup

2.2. Measurements and calculations

Open- and closed-circuit modes of three tubular MFCs operated and their voltages were recorded by a multimeter device (VC9805 Zhangzhou Weihua Electronic Co., Ltd., Fujian, China). The current (I) passing through the circuit was readily obtained using the well-known Eq. (1):

$$I = V/R_{ex} \quad (1)$$

where V is the voltage (V) and R_{ex} (1000 Ω) is the external resistance. Subsequently, the data for polarization were produced by varying the external resistances from 17 to 44000 Ω. The resulting voltages were recorded after stabilization. The Power Density (PD) and Current Density (CD) can be calculated through the following equations (Eq. 2 and Eq. 3):

$$PD = \frac{V^2}{R_{ext}A} \quad (2)$$

$$CD = \frac{V}{R_{ext}A} \quad (3)$$

where V, R_{ex}, and A represent the voltage (V), external resistance (Ω), and the effective surface area of proton transfer (m^2), respectively.

An instrument according to a standard method (photometer AL250 & CSB/COD-Reactor AL38, AQUALYTIC, Dortmund, Germany) was used to measure the Chemical Oxygen Demand (COD) for the fresh and treated wastewaters. Moreover, a Manometric BOD Measuring device (OxiTop®IS, USA) was used to obtain the Biological Oxygen Demand (BOD).

The Coulombic Efficiency (CE) was obtained using Eq. (4) [2].

$$CE(\%) = \frac{M\int_0^t I\,dt}{F\,b\,v_{An}\,\Delta COD} \quad (4)$$

where F represents Faraday's constant; b = 4 is the number of exchanged electrons per each mole of reacted oxygen; ΔCOD is the difference between inlet and outlet COD of anolyte; v_{An} is the volume of the anode compartment, and M represents the oxygen molecular weight.

2.3. Experimental design

The D-optimal method is one of the most useful techniques in the Response Surface Methodologies (RSM). D-optimal technique is well used for the curve fitting of complex problems, optimization, and experimental investigations. In addition, this method is applied to the chronological experimentation.

Several factors can influence the overall performance of microbial fuel cells. However, based on the experimental results of the previous work [20], three independent factors of anolyte flow rate, proton exchange layers arrangements, and flow pattern of anodic and cathodic influents were adopted as the most influencing parameters to be optimized using RSM. The independent parameters including flow rate of anolyte (2.9 to 6.9 (ml/min) at five levels), types and orders of the proton exchange layers (3 types, namely NC, JC, AL), and flow pattern in the cathode and anode compartments (2 patterns, i.e., co-current and counter-current) along with their experimental levels are shown in Table 1.

Table 1. Factors and levels of the experimental designs

Variables	Symbol	Variable levels				
Flow rate (ml/min)	A	2.9	3.9	4.9	5.9	6.9
Types and order of exchange layers	B	NC-JC	NC-JC-AL		NC-AL-JC	
Relative flow pattern of cathode and anode influents	C	Co-current		Counter-current		

The Maximum Power Density (MPD, mW/m^2) and the Coulombic Efficiency (CE, %) of the MFCs were defined as the responses of the statistical design. It is important to notice

that if RSM is not used in many experiments, higher expenses occur. Here, the nylon-cloth (NC), J-cloth (JC), and the absorbent layer (AL) of artificial rayon constitute the layers of the proton exchange medium in the MFCs with three distinct arrangements. The experimental designs and the RSM analysis were performed by means of Design-Expert software (version 8.0.0).

The experimental design of this study is represented in Table 2. The main responses in the statistical analysis are the MPD and CE of the microbial fuel cells. Table 2 shows the internal resistance of the microbial fuel cells for each experiment, which have been estimated from the concentration polarization plots. However, the internal resistance cannot be identified as the third independent response of RSM design, owing to its interconnection with the power density of microbial fuel cell.

Table 2. Design arrangement and experimental results for three responses of RSM design

Run	A: Anolyte flow rate (ml/min)	B: Types and orders of proton exchange layers	C: Flow patterns	Internal resistance (Ω)	R1: MPD (mW/m^2)	R2: CE (%)
1	2.9	NC-AL-JC	counter-current	546.3	197.659	1.8173
2	4.9	NC-AL-JC	co-current	383.1	222.700	3.7127
3	2.9	NC-JC	co-current	445.1	196.216	3.4912
4	6.9	NC-JC	counter-current	376.8	258.664	4.5321
5	3.9	NC-JC-Al	co-current	459.2	215.437	4.4341
6	2.9	NC-JC	co-current	445.2	225.601	3.1653
7	6.9	NC-JC-Al	co-current	343.8	276.915	4.0810
8	2.9	NC-JC-Al	counter-current	519.4	179.534	3.6810
9	4.9	NC-JC-Al	counter-current	584.2	188.260	3.3306
10	3.9	NC-JC	counter-current	476.9	203.812	3.8721
11	5.9	NC-JC	co-current	329.3	224.002	4.3174
12	6.9	NC-JC-Al	counter-current	344.2	274.692	4.4162
13	6.9	NC-AL-JC	co-current	323.9	285.895	4.9675
14	5.9	NC-JC	co-current	329.4	252.382	4.2385
15	6.9	NC-JC	counter-current	376.7	285.496	4.2995
16	5.9	NC-AL-JC	counter-current	410.1	212.175	1.6427
17	2.9	NC-AL-JC	co-current	433.4	201.272	3.2639

3. RESULTS AND DISCUSSION

3.1. Results for wastewater treatment

The COD and BOD of input wastewater were 1220 and 560 (mg/lit), respectively, with the BOD/COD ratio of 0.46. The BOD of the output stream was measured to be 95 (mg/lit), with 83 % percent of treatment, which seems to be an acceptable result [33].

3.2. Statistical optimization results

Microbial fuel cells are complex systems in which many factors can influence their performance. However, the performance of MFC systems can be optimized from different viewpoints such as maximizing the power generation, wastewater treatment, or current production. In the present study, two most important parameters of MPD and CE were adopted as the main responses of statistical optimization. Two distinct analyses of variance (ANOVA) were separately done for each response of RSM optimization, which is described in the following sections thoroughly.

3.2.1. The first response of RSM optimization: MPD

The results of ANOVA for MPD (Table 3) reveal that only A (flow rate), C (flow pattern), and A^2 can significantly affect (p-value < 0.05) the power generation of the MFCs. However, the order of separator layers (B) was not recognized as a significant parameter in the power production of the MFCs. Moreover, these results indicated that the influent flow rate of anolyte (A) was the most prominent parameter in the MPD of the MFCs.

The low p-value obtained for the model parameter indicates that the obtained model for the response is significant in terms of statistical analysis and there is a chance of 0.01 % in which the high amount of the model F-value (33.24) can occur due to existing noise. In addition, a value of 0.8847 was found for the coefficient of determination (R^2). Also, reasonable agreement between "Adjusted R^2" (0.8580) and "Predicted R^2" (0.8063) confirmed that the observed and predicted values had a good correlation. Comparison of the residual and pure errors in terms of replicated experimental design is obtained by the "lack of fit tests". In this regard, the p-values > 0.05 mean that there is an insignificant lack of fit. Furthermore, "Adequate

Precision" of 14.717, which presents the signal-to-noise ratio, implies an adequate signal. Overall, the obtained model can acceptably be employed to navigate the design space. Finally, an expression was produced mathematically from this statistical analysis. Equation 5 shows the mathematical expression in terms of the codded significant factors, and Equation 6 points to the correlation between the MPD and the actual factors of the analysis as follows:

$$MPD = 207.40 + 37.42 \times A - 8.30 \times C + 30.92 \times A^2 \quad (5)$$

$$MPD = k - 57.042 \times (F) + 7.729(F)^2 \quad (6)$$

where F represents the flow rate of anolyte and k is a constant value that is equal to 309.625 for co-current and 293.023 for counter-current flow patterns, respectively.

Table 3. The ANOVA analysis for the maximum power density (MPD) of the MFCs (the first response of RSM design)

Source	Sum of squares	df	Mean square	F-value	p-value	
Model	17999.26	3	5999.75	33.24	< 0.0001	significant
A-flow rate	15506.08	1	15506.08	85.90	< 0.0001	
C-flow pattern	1148.36	1	1148.36	6.36	0.0255	
A^2	2726.66	1	2726.66	15.11	0.0019	
Residual	2346.67	13	180.51			
Lack of fit	1152.22	10	115.22	0.29	0.9407	not significant
Pure error	1194.45	3	398.15			
Cor total	20345.93	16				
R^2= 0.8847 Adj. R^2= 0.8580						

3.2.2. The second response of RSM optimization: Coulombic Efficiency (CE)

The analysis of variance (ANOVA) for the CE has been done separately as the second response of the statistical optimization (Table 4). The results of this analysis reveal that all of three independent variables including anolyte flow rate (A), the orders of proton exchange layers (B), and relative flow patterns (C) of the anolyte and catholyte influents have statistically significant influence (p-value <0.05) on the CE of the MFCs. Interestingly, the orders of proton exchange layers (B), not recognized as a significant parameter in the analysis of variance of the first response, i.e., power density, has the highest F-value now. Therefore, although the orders of proton exchange layers may not have a significant impact on the power generation proficiency of microbial fuel cells, it can, however, control the rate of oxygen transportation between the cathode and anode compartment and hence, greatly affect the CE of the MFC systems. Comparison of the average values of coulombic efficiency for different arrangements shows that the addition of absorbent layer after the J-cloth improves the coulombic efficiency by about 15 %.

The prediction model for the CE has been modified using a reciprocal square root transformation to improve the normality of data. Results of ANOVA show that the resulting model is statistically significant. Acceptable proximity of R^2 (0.9436) value to 1.0 along with the agreement of the adjusted R^2 (0.9098) and the predicted R^2 (0.8868) values confirmed the model adequacy. Moreover, insignificant “lack of fit” along with the high value of "Adequate Precision" (17.622) indicates a sufficient signal-to-noise ratio and model adequacy.

Table 4. ANOVA for the coulombic efficiency (CE) of the MFCs as the second response of RSM

Source	Sum of squares	df	Mean square	F-value	p-value	
Model	0.12	6	0.021	27.90	< 0.0001	significant
A-flow rate	4.495E-003	1	4.495E-003	6.05	0.0337	
B-layers arrangement	0.046	2	0.023	30.89	< 0.0001	
C-flow pattern	0.020	1	0.020	26.76	0.0004	
BC	0.048	2	0.024	32.24	< 0.0001	
Residual	7.432E-003	10	7.432E-004			
Lack of fit	7.012E-003	7	1.002E-003	7.15	0.0671	not significant
Pure error	4.204E-004	3	1.401E-004			
Cor total	0.13	16				
R^2= 0.9436 Adj. R^2= 0.9098						

Finally, the following mathematical correlation was derived to predict the coulombic efficieny of microbial fuel cells based on the significant parameters of “proton exchange layers” (B), “flow rate” (A), and “flow patterns” (C) regarding the coded (Eq. 7) and the actual factors (Eq. 8).

$$\frac{1}{\sqrt{CE}} = 0.55 - 0.021 \times A - 0.044 \times B[1] + 0.091 \times B[2] + 0.040 \times C - 0.028 \times B[1]C + 0.078 \times B[2]C \quad (7)$$

$$\frac{1}{\sqrt{CE}} = C_1 - 0.0106 \times F \quad (8)$$

where F is the flow rate of anolyte influent and different values of C1 constant in Eq. 8 for each categorical factor are mentioned in Table 5.

Table 5. Constant values of correlated expressions for CE (Eq. 8)

Flow pattern (C)	Proton exchange layers arrangements (B)	C_1 (Eq.8)
Co-current	NC-JC-AL	0.5422
Counter-current	NC-JC-AL	0.5669
Co-current	NC-AL-JC	0.5708
Counter-current	NC-AL-JC	0.8077
Co-current	NC-JC	0.5627
Counter-current	NC-JC	0.5418

3.3. Investigation of the effects of the prominent parameters and their interactions

3.3.1. The effect of proton exchange layer arrangements

Microbial fuel cells are useful and eco-friendly technologies that can generate electricity from various waste materials. Generally, the organic matters are biologically degraded in the anode chamber using the exoelectrogens, and the produced electrons are transferred via the external circuit to react with the final electron-acceptor at the cathode (usually oxygen). The proton exchange membrane between the anode and cathode chambers transfers the generated protons in the anode to the cathode. It also provides a distance as close as possible between the electrodes and at the same time, prevents the short-circuiting, crosses the species between the chambers, and maintains anaerobic anodic environment by controlling the oxygen migration from the cathode to the anode compartment.

However, the objective of this paper is to substitute common highly expensive polymeric proton exchange membranes, with super-low-cost cloth layers. In this regard, the effect of different arrangements of three layers of nylon cloth (NC), J-cloth (JC), and glass fiber (GF) on the overall performance of MFCs was investigated statistically. The results of our previous research revealed that the placement of J-cloth fabric after the NC layer could sufficiently block the oxygen transportation between the MFC chambers due to the formation of good biofilm layer. However, the arrangement of NC-JC-GF was the best separator arrangement design since the addition of GF layer after the JC layer improved the power density by the 5.15 % compared to the NC-JC design [20]. In the present study, the application of another adsorbent layer, instead of the GF layer, after the j-cloth was examined thoroughly. Therefore, different arrangements of three layers of NC, JC, and absorbent rayon layer (AL) were investigated statistically. The power generation performance, cost, and coulombic efficiency of the present separator electrode assemblies were compared with the other low-cost porous fabric separators in Table 6.

Table 6. Comparison of the power output, coulombic efficiency, and cost of porous fabric separators

Separator	Thickness (mm)	Pore size (µm)	$K_o \times 10^{-4}$ (cm/s)	R_{ohm} (Ω)	R_{in} (Ω)	CE (%)	PD (mW/m^2)	Cost ($/$m^2$)	PO (mW/$)	Ref.
NWF1	0.13	2.01	Nd	60.1 ± 8.7	43 ± 2	Nd	40.8 ± 7.2	2	20.4	[34]
NWF2	0.18	1.78	Nd	59.2 ± 1.2	53 ± 6	Nd	79.2 ± 6.5	3	26.4	
NWF3	0.25	1.81	Nd	72.1 ± 9.5	37 ± 1	Nd	62.7 ± 6.9	4	15.6	
NWF4	0.13	1.21	7.0	46.9 ± 6.5	51 ± 7.5	20	97.0 ± 7.5	2	48.5	
Nafion 117	0.19	Nd	6.7	73.1 ±8.3	93 ± 2	22	57.5 ± 3.9	1400	0.04	
NWF-PP80	0.49	30	0.37 ± 0.2	9.29	Nd	22	Nd	0.57	Nd	[34]
NWF-PP100	0.54	42	0.73 ± 0.6	9.50	Nd	18	117	0.57	Nd	
PPS	0.52	40	0.75 ± 0.7	9.51	Nd	11	102	8.33	Nd	
S-PPS	0.54	44	0.72 ± 0.2	3.53	Nd	14	190	9.2	Nd	
CMI-7000	0.46	4-12	0.2	9.68	Nd	16	78	166	Nd	
Nafion 117	0.19	5×10^{-3}	0.75	3.13	Nd	19	24	2300	Nd	
J-Cloth	0.3	Nd	29.0	0.21± 0.08	38.1± 0.1	~40	786 ± 23	Nd	Nd	[34]
GF 1	1	Nd	0.50	2.26 ±0.1	38.1± 0.1	~80	791 ± 69	Nd	Nd	
GF 0.4	0.4	Nd	0.75	2.39 ± 0.3	40.1 ± 0.4	~78	623 ± 4	Nd	Nd	
CMI-7000	0.46	Nd	0.94	3.78 ± 0.4	131.7 ± 8.4	Nd	267 ± 22	Nd	Nd	
Nylon 0.2	0.170	0.2	Nd	Nd	84.6	70	443±27	Nd	Nd	[34]
Nylon 0.45	0.170	0.45	Nd	Nd	57.3	63	650 ± 7	Nd	Nd	
Nylon 10	0.045	10	Nd	Nd	41.4	55	769±65	Nd	Nd	
Nylon 60	0.050	60	Nd	Nd	39.5	45	816 ± 34	Nd	Nd	
Nylon 100	0.080	100	Nd	Nd	37.3	41	908 ± 24	Nd	Nd	
Nylon 160	0.100	160	Nd	Nd	35.7	31	941±47	Nd	Nd	
GF 0.7	0.380	0.7	Nd	Nd	40.4	56	732 ± 48	Nd	Nd	
GF 1	0.700	1.0	Nd	Nd	42.3	60	716 ±60	Nd	Nd	

GF 2	0.380	2.0	Nd	Nd	39.6	55	779 ±43	Nd	Nd	
NC-JC	0.15	Nd	Nd	Nd	576.09	6.03 ± 0.3	267.17 ± 30.6	7	38.2	[34]
NC-JC-GF	0.55	Nd	Nd	Nd	562.09	5.78 ± 0.3	281.30 ± 32.3	7.32	38.4	
NC-JC	1.5	Nd	Nd	Nd	397.1 ± 59	4.7	285.49	7	40. 8	This study*
NC-JC-AL	4.5	Nd	Nd	Nd	450.2 ± 106	4.08	276.91	~7.5	36.9	
NC-AL-JC	4.5	Nd	Nd	Nd	419.4 ± 82	4.26	285.89	~7.5	38.1	

Nd: not determined; NWF: non-woven fabric; NC: Nylon cloth, JC: J-cloth, GF: Glass fiber; AL: adsorbent layer.

* The highest values of power density obtained for each arrangement are provided in this table for comparison with the other separator types. The detailed results of experiments are listed in Table 2.

Figure 3 compares the results of two MFC experiments with different arrangements of NC-JC and NC-JC-AL. The other parameters of flow-patterns and flow-rate were similar in these experiments which were adjusted to counter-current and 6.9 ml/min, respectively. According to Figure 3, there is no marked difference in the open circuit voltages, currents, and polarization results of these MFCs. However, comparing the concentration polarization curves in Figure 3C revealed that although the overpotential and concentration losses were almost similar for these two arrangements, by taking into account the slope of the middle part of plots, the ohmic losses for the NC-JC-Al were slightly lower than the values for NC-JC. Altogether, unlike the glass fiber, the addition of rayon layer after the JC could not significantly improve the performance of MFC, as expected. However, as stated in the previous sections, ANOVA analysis confirmed that these different arrangements of proton exchange layers had only statistically significant impact on the CE of MFCs (p-value <0.05) and marginal differences in the maximum power densities of MFCs were not statistically significant.

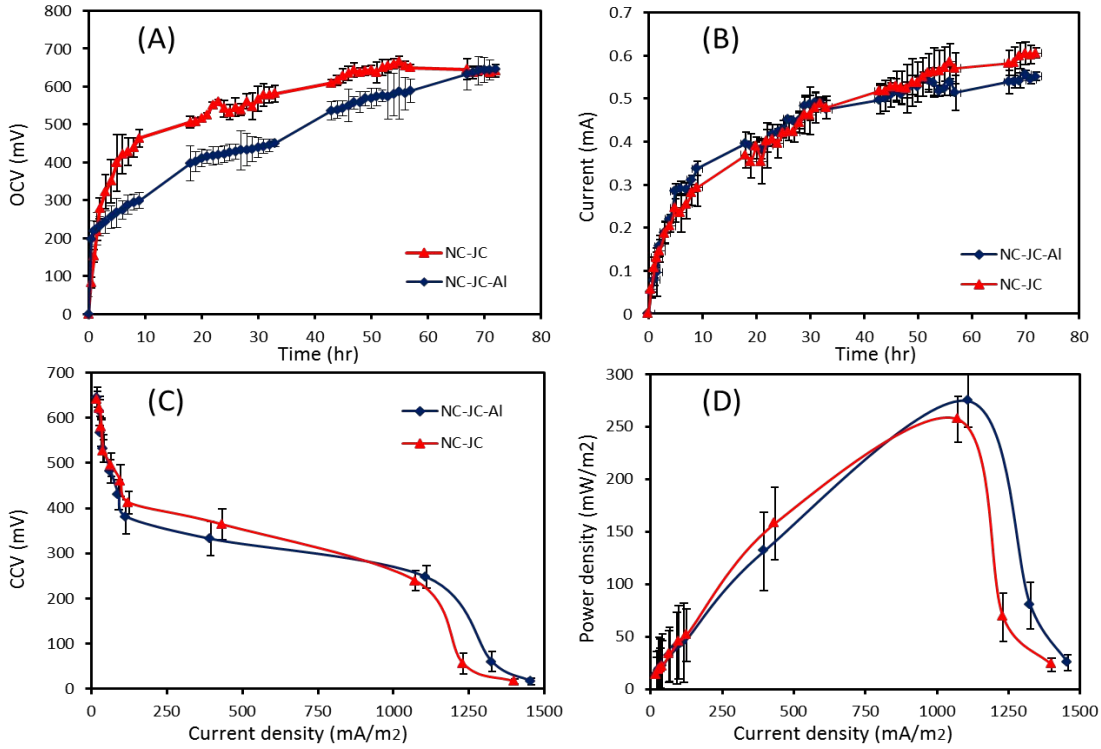

Figure 3. A comparison of the results of two experiments with different proton exchange layers of NC-JC and NC-JC-AL: (A) open circuit voltage, (B) current production, (C) closed circuit voltage, and (D) power density

Furthermore, the combined effects of independent variables on the two responses of RSM optimization were investigated as well as their individual effects. Figure 4 illustrates the combined effects of layer arrangements (B) and flow patterns of influents (C) on the two responses of MPD and CE.

Statistical analysis showed that although different arrangements of the above-mentioned cloths had no significant effect on the maximum generated power as well as open-circuit voltages of MFCs, it can seriously control the oxygen crossover between the chambers and affect the current production and CE of MFCs. Nevertheless, as can be seen in Figure 4B, the effect of layer arrangements on the CE was more pronounced in the counter-current mode of influents. It seems that higher pressure differences occurred in the counter-current mode result in the more oxygen passage across the separator layers, which hindered the performance of MFCs and decreased the CE. Moreover, the lowest CE was achieved when the absorbent rayon layer (AL) was placed next to the nylon cloth (NC) layer instead of J-Cloth (JC) since the high-porous rayon layer could not block the oxygen transfer

through the separator adequately. This fundamental role of J-cloth in the control of oxygen transportation rate is consistent with the results of our previous study [20].

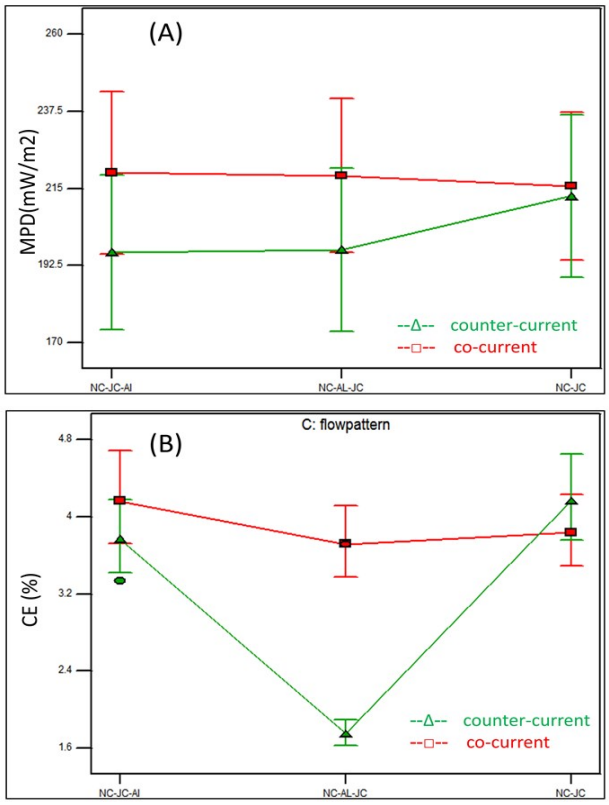

Figure 4. Combined effects of different separator layers (factor B) and flow patterns (factor C) on the two responses of RSM optimization: (A) MPD and (B) CE; the red squares and green triangles represent the co-current and counter-current modes, respectively

3.3.2. The effect of wastewater flow rate or Hydraulic Retention Time (HRT)

It is well known that the adoption of the appropriate HRT of anolyte in the anode compartment has a significant effect on the performance of MFCs with continuous flow mode, because it must be consistent with the generation rate of anodic bacteria and provide enough organic substrates for them. In this study, like many others, different anodic HRTs have been adjusted by changing the flow rates of influent wastewater.

The flow rate of wastewater effect on the two responses of MPD and CE is depicted in Figure 5. Consistent with our previous work, both the maximum power density and CE of MFCs were enhanced by increasing the flow rate or, in other words, by decreasing the wastewater HRT in the anode compartment. The rate of altering the responses by the change of wastewater flow rate was obviously different. The MPD of MFCs increased polynomial, whereas CE had a linear growth by increasing the flow rate of wastewater.

3.3.3. The effect of influent flow patterns on the performance of MFCs

Both responses of the statistical optimization are presented in Figure 6, which are affected by different modes of co-current and counter-current operations. Consistent with the results of our previous research, MFCs have better performance in the co-current configuration than the counter-current in terms of both the power production and CE. This priority of co-current over the counter-current mode is probably due to higher trans-membrane pressure and more oxygen crossover between the chambers in the counter-current design of MFCs, as described previously [20].

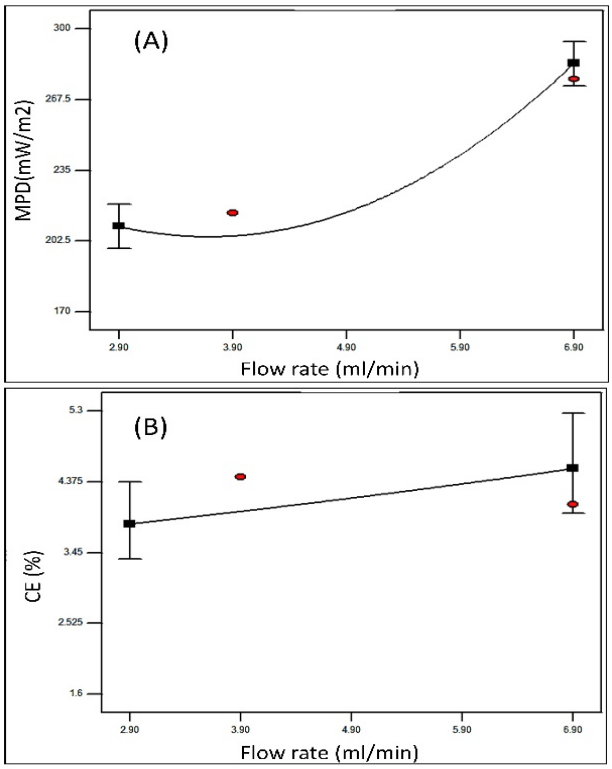

Figure 5. The effect of influent wastewater flow rate on (A) MPD and (B) CE of microbial fuel cells; red circles indicate the experimental design points

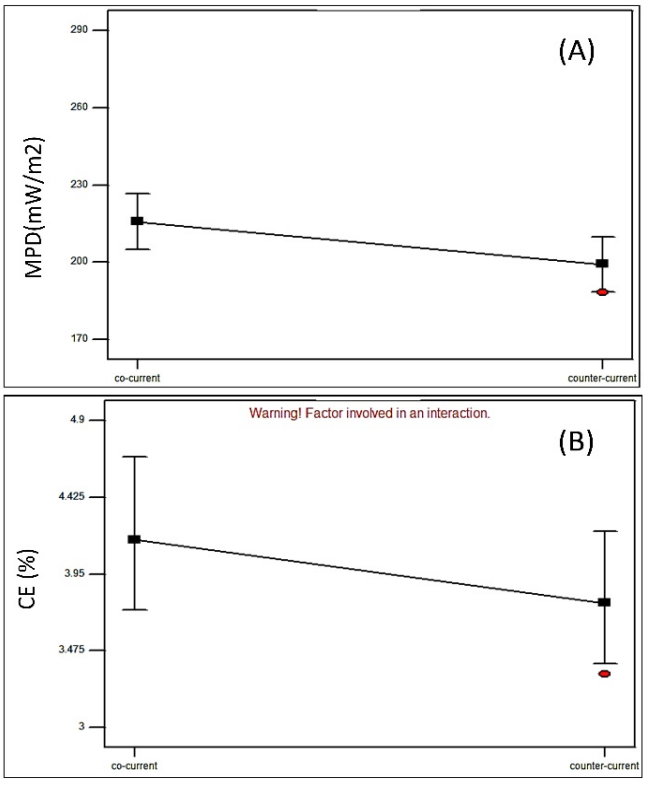

Figure 6. The effect of co-current and counter-current modes on the two responses of (A) MPD and (B) CE of MFCs; red circles indicate the experimental design points

4. CONCLUSIONS

In the present study, three more important operating parameters of influent flow patterns, different proton exchange layers, and the hydraulic retention time (HRT) of used wastewater in the anode compartment were statistically optimized by using the D-optimal-based response surface methodology (RSM). Two independent responses of maximum power density (MPD) and CE of MFCs were adopted for this optimization and two distinct ANOVA analyses were done for them. Statistical analyses confirmed that although different arrangements of nylon cloth, J-cloth, and absorbent rayon layer (AL) did not have a significant impact on the power production, it could critically influence the oxygen transfer rate between the anode and cathode chambers and thereby the CE of MFCs. Among the three configurations of NC-JC, NC-JC-AL, and NC-AL-JC, the first design of NC-JC-Al was the best arrangement. However, the addition of absorbent rayon layer after the J-cloth could not improve the MFC performance considerably. Since the application of rayon layer, with extremely high porosity, just increased the electrode distance without sufficient enhancement of the oxygen barrier property of separator. The MFC with NC-JC-AL assembly generated almost the same power density, but 8.2 % higher CE than the NC-JC design.

On the other hand, MFCs had superior performance in the co-current flow pattern compared to counter-current in terms of both the power production and CE. Moreover, investigation of the combined parameters effects revealed that the effect of separator layer arrangements was more pronounced in the counter-current flow patterns, owing to its higher-pressure difference and more oxygen penetration between the MFC chambers. Furthermore, the higher flow rates of wastewater improved the MFC performance due to the sufficiency of the organic substrate for the growth of anodic bacteria. Overall, the best conditions based on this optimization study were the co-current flow pattern, NC-JC-Al separator arrangement, and the anolyte flow rate of 6.9 (ml/min).

5. ACKNOWLEDGMENT

This research was supported by the University of Sistan and Baluchestan.

REFERENCES

1. Logan, B.E., Microbial fuel cells, John Wiley & Sons Inc., Hoboken, New Jersey, (2007).
2. Logan, B.E., Hamelers, B., Rozendal, R., Schroder, U., Keller, J., Freguia, S., Aelterman P., Verstraete W. and Rabaey K., "Microbial fuel cells: Methodology and technology", ***Environmental Science and Technology***, Vol. 40, No. 17, (2006), 5181-5192. (https://doi.org/10.1021/es0605016).
3. Lovley, D.R., "The microbe electric: Conversion of organic matter to electricity", ***Current Opinion in Biotechnology***, Vol. 19, No. 6, (2008), 564-571. (https://doi.org/10.1016/j.copbio.2008.10.005).
4. El Haj Assad, M., Khosravi, A., Malekan, M., Rosen, M.A. and Nazari, M.A., "Chapter 14 - Energy storage", Design and performance optimization of renewable energy systems, Academic Press, (2021), 205-219. (https://doi.org/10.1016/B978-0-12-821602-6.00016-X).
5. Logan, B.E., "Exoelectrogenic bacteria that power microbial fuel cells", ***Nature Reviews Microbiology***, Vol. 7, No. 5, (2009), 375-381. (https://doi.org/10.1038/nrmicro2113).
6. Tan, W.H., Chong, S., Fang, H.-W., Pan, K.-L., Mohamad, M., Lim, J.W., Tiong, T.J., Chan, Y.J., Huang, C.-M. and Yang, T.C.-K., "Microbial fuel cell technology—A critical review on scale-up issues", ***Processes***, Vol. 9, No. 6, (2021), 985. (https://doi.org/10.3390/pr9060985).
7. Kataki, S., Chatterjee, S., Vairale, M.G., Sharma, S., Dwivedi, S.K. and Gupta, D.K., "Constructed wetland, an eco-technology for wastewater treatment: A review on various aspects of microbial fuel cell integration, low temperature strategies and life cycle impact of the technology", ***Renewable and Sustainable Energy Reviews***, Vol. 148, No. (2021), 111261. (https://doi.org/10.1016/j.rser.2021.111261).
8. You, S., Zhao, Q., Zhang, J., Jiang, J. and Zhao, S., "A microbial fuel cell using permanganate as the cathodic electron acceptor", ***Journal of Power Sources***, Vol. 162, No. 2, (2006), 1409-1415. (https://doi.org/10.1016/j.jpowsour.2006.07.063).
9. Fornero, J.J., Rosenbaum, M., Cotta, M.A. and Angenent, L.T., "Microbial fuel cell performance with a pressurized cathode chamber", ***Environmental Science & Technology***, Vol. 42, No. 22, (2008), 8578-8584. (https://doi.org/10.1021/es8015292).
10. Oh, S., Min, B. and Logan, B.E., "Cathode performance as a factor in electricity generation in microbial fuel cells", ***Environmental Science & Technology***, Vol. 38, No. 18, (2004), 4900-4944. (https://doi.org/10.1021/es049422p).
11. Rabaey, K. and Verstraete, W., "Microbial fuel cells: Novel biotechnology for energy generation", ***Trends in Biotechnology***, Vol. 23, No. 6, (2005), 291-298. (https://doi.org/10.1016/j.tibtech.2005.04.008).
12. Miroliaei, M.R., Samimi, A., Mohebbi-Kalhori, D., Khorram, M. and Qasemi, A., "Competition between *E. coli* and *Shewanella sp.* for electricity generation in air cathode MFC in presence of methylene blue as artificial mediator", ***Environmental Progress & Sustainable Energy***, Vol. 34, No. 4, (2015), 1097-1105. (https://doi.org/10.1002/ep.12111).
13. Zhuwei, D.U., Haoran, L.I. and Tingyue, G.U., "A state of the art review on microbial fuel cells: A promising technology for wastewater treatment and bioenergy", ***Biotechnology Advances***, Vol. 25, No. 5, (2007), 464-482. (https://doi.org/10.1016/j.biotechadv.2007.05.004).
14. Oh, S.T., Kim, J.R., Premier, G.C., Lee, T.H., Kim, C. and Sloan, W.T., "Sustainable wastewater treatment: How might microbial fuel cells contribute", ***Biotechnology Advances***, Vol. 28, No. 6, (2010), 871-881. (https://doi.org/10.1016/j.biotechadv.2010.07.008).
15. Ouitrakul, S., Sriyudthsak, M., Charojrochkul, S. and Kakizono, T., "Impedance analysis of bio-fuel cell electrodes", ***Biosensors and Bioelectronics***, , Vol. 23, No. 5, (2007), 721-772. (https://doi.org/10.1016/j.bios.2007.08.012).
16. Zhou , M.C., Luo , M.J., He, H. and Jin, T., "An overview of electrode materials in microbial fuel cells", ***Journal of Power Sources***, Vol. 196, No. 10, (2011), 4427-4443. (https://doi.org/10.1016/j.jpowsour.2011.01.012).
17. Khalili, H.-B., Mohebbi-Kalhori, D. and Afarani, M.S., "Microbial fuel cell (MFC) using commercially available unglazed ceramic wares: Low-cost ceramic separators suitable for scale-up", ***International Journal of Hydrogen Energy***, Vol. 42, No. 12, (2017), 8233-8241. (http://dx.doi.org/10.1016/j.ijhydene.2017.02.095).
18. Yousefi, V., Mohebbi-Kalhori, D. and Samimi, A., "Ceramic-based microbial fuel cells (MFCs): A review", ***International Journal of Hydrogen Energy***, Vol. 42, No. 3, (2017), 1672-1690. (https://doi.org/10.1016/j.ijhydene.2016.06.054).
19. Li, W.-W., Sheng, G.-P., Liu, X.-W. and Yu, H.-Q., "Recent advances in the separators for microbial fuel cells", ***Bioresource Technology***, Vol. 102, No. 1, (2011), 244-252. (https://doi.org/10.1016/j.biortech.2010.03.090).
20. Yousefi, V., Mohebbi-Kalhori, D., Samimi, A. and Salari, M., "Effect of separator electrode assembly (SEA) design and mode of operation on the performance of continuous tubular microbial fuel cells (MFCs)", ***International Journal of Hydrogen Energy***, Vol. 41, No. 1, (2016), 597-606. (https://doi.org/10.1016/j.ijhydene.2015.11.018).
21. Yousefi, V., Mohebbi-Kalhori, D. and Samimi, A., "Equivalent electrical circuit modeling of ceramic-based microbial fuel cells using the electrochemical impedance spectroscopy (EIS) analysis", ***Journal of Renewable Energy and Environment (JREE)***, Vol. 6, No. 1, (2019), 21-28. (https://doi.org/10.30501/JREE.2019.95555).
22. Cheraghipoor, M., Mohebbi-Kalhori, D., Noroozifar, M. and Maghsoodlou, M.T., "Comparative study of bioelectricity generation in a microbial fuel cell using ceramic membranes made of ceramic powder, Kalporgan's soil, and acid leached Kalporgan's soil", ***Energy***, Vol. 178, (2019), 368-377. (https://doi.org/10.1016/j.energy.2019.04.124).
23. Cheraghipoor, M., Mohebbi-Kalhori, D., Noroozifar, M. and Maghsoodlou, M.T., "Production of greener energy in microbial fuel cell with ceramic separator fabricated using native soils: Effect of lattice

and porous SiO_2", ***Fuel***, Vol. 284, (2021), 118938. (https://doi.org/10.1016/j.fuel.2020.118938).

24. Rodríguez, J., Mais, L., Campana, R., Piroddi, L., Mascia, M., Gurauskis, J., Vacca, A. and Palmas, S., "Comprehensive characterization of a cost-effective microbial fuel cell with Pt-free catalyst cathode and slip-casted ceramic membrane", ***International Journal of Hydrogen Energy***, Vol. 46, No. 51, (2021). (https://doi.org/10.1016/j.ijhydene.2021.01.066).
25. Yousefi, V., Mohebbi-Kalhori, D. and Samimi, A., "Application of layer-by-layer assembled chitosan/montmorillonite nanocomposite as oxygen barrier film over the ceramic separator of the microbial fuel cell", ***Electrochimica Acta***, Vol. 283, (2018), 234-247. (https://doi.org/10.1016/j.electacta.2018.06.173).
26. Yousefi, V., Mohebbi-Kalhori, D. and Samimi, A., "Start-up investigation of the self-assembled chitosan/montmorillonite nanocomposite over the ceramic support as a low-cost membrane for microbial fuel cell application", ***International Journal of Hydrogen Energy***, Vol. 45, No. 7, (2020), 4804-4820. (https://doi.org/10.1016/j.ijhydene.2019.11.216).
27. Zhang, F., Ahn, Y. and Logan, B.E., "Treating refinery wastewaters in microbial fuel cells using separator electrode assembly or spaced electrode configurations", ***Bioresource Technology***, Vol. 152, (2014), 46-52. (https://doi.org/10.1016/j.biortech.2013.10.103).
28. Ahn, Y. and Logan, B.E., "Domestic wastewater treatment using multi-electrode continuous flow MFCs with a separator electrode assembly design", ***Applied Microbiology and Biotechnology***, Vol. 97, No. 1, (2013), 409-416. (https://doi.org/10.1007/s00253-012-4455-8).
29. Steinberg, D.M. and Bursztyn, D., "Response surface methodology in biotechnology", ***Quality Engineering***, Vol. 22, No. 2, (2010), 78-87. (https://doi.org/10.1080/08982110903510388).
30. Yousefi, V. and Kariminia, H.-R., "Statistical analysis for enzymatic decolorization of acid orange 7 by *Coprinus cinereus* peroxidase", ***International Biodeterioration & Biodegradation***, Vol. 64, No. 3, (2010), 245-252. (https://doi.org/10.1016/j.ibiod.2010.02.003).
31. Kariminia, H.-R. and Yousefi, V., "Statistical optimization of reactive blue 221 decolorization by fungal peroxidise", Water production and wastewater treatment, NOVA publisher, (2011), Chap. 12, 215-224.
32. Raychaudhuri, A. and Behera, M., "Review of the process optimization in microbial fuel cell using design of experiment methodology", ***Journal of Hazardous, Toxic, and Radioactive Waste***, Vol. 24, No. 3, (2020), 04020013. (https://doi.org/10.1061/(ASCE)HZ.2153-5515.0000503).
33. Jang, J.K., Pham, T.H., Chang, I.S., Kang, K.H., Moon, H. and Chok, S., "Construction and operation of a novel mediator-and membraneless microbial fuel cell", ***Process Biochem***, Vol. 39, No. 8, (2004), 1007-1012. (https://doi.org/10.1016/S0032-9592(03)00203-6).
34. Choi, S., Kim, J.R., Cha, J., Kim, Y., Premier, G.C. and Kim, C., "Enhanced power production of a membrane electrode assembly microbial fuel cell (MFC) using a cost effective poly [2,5-benzimidazole] (ABPBI) impregnated non-woven fabric filter", ***Bioresource Technology***, Vol. 128, (2013), 14-21. (https://doi.org/10.1016/j.biortech.2012.10.013).